IL-23 Inhibits Melanoma Development by Augmenting DNA Repair and Modulating T-cell Subpopulations

Tahseen H. Nasti[*,†], **J. Barry Cochran**[*], **Raj V Vachhani**[*], **Kristopher McKay**[*], **Yuko Tsuruta**[*], **Mohammad Athar**[*], **Laura Timares**[*,‡], and **Craig A. Elmets**[*,‡,§]

[*]The Department of Dermatology, University of Alabama at Birmingham School of Medicine, Birmingham Alabama

[§]The Birmingham VA Medical Center, Birmingham, Alabama, USA.

Abstract

In animal models, IL-12 and IL-23 participate in the development of malignant neoplasms of keratinocytes. However, the role of these cytokines in pigmented lesion development and their progression to melanoma has received little attention. IL-12p35, IL-23p19, and IL-12/IL-23p40 knockout mice on a C3H/HeN background, subjected to a melanomagenesis protocol, demonstrated profound differences in susceptibility to nevus initiation, transformation, tumorigenicity and metastatic potential. IL-23 was found to be essential for melanocyte homeostasis, whereas IL-12 supported nevus development. A direct action of IL-23 on primary melanocytes, shown to be IL-23R+, demonstrated that DNA repair of damaged melanocytes requires IL-23. Further, IL-23 modulated the cutaneous microenvironment by limiting regulatory T cells and IFNγ and inhibiting IL-10 production. Neutralizing antibody to IFNγ, but not IL-17, inhibited nevus development (p<0.01).

Keywords

IL-23; IL-12; Nevi; Melanoma; DMBA

Introduction

Melanomas are an aggressive, treatment resistant cancer of melanocytes (1, 2) that often begin as benign pigmented nevi. Families have been described who often have >50 nevi, many of which have atypical clinical and pathological features (3). Individuals from these families have a substantially increased risk of melanomas and frequently have multiple melanomas. The melanomas in these patients often begin at a younger age (3-6). Up to 40% of melanoma prone families have germ-line mutations in the CDKN2A gene (4). In families with this syndrome, the melanomas do not have a clear relationship to ultraviolet radiation. CDKN2A mutations are present in all melanocytes, but not all melanocytes go on to become

Correspondence to Department of Dermatology, EFH 414, Birmingham AL-35294, celmets@uabmc.edu; timares@uab.edu, Phone 205-934-5188.
[†]Current Address. Department of Immunology and Microbiology, Emory University, Atlanta, GA.
[‡]Co-principal investigators.

melanomas, because dysplastic nevi, and their progression to melanomas, require additional molecular hits. Among the other genes commonly mutated in melanoma is the ras gene (7). Activating mutations in codon 61 of N-*ras* have been identified in 95% of primary melanomas in these patients; these same mutations are also present in dysplastic nevi and metastatic melanomas (7). Activating N-*ras* mutations have been found in congenital melanocytic nevi and H-*ras* mutations have been identified in Spitz nevi (8), highlighting their importance in the genesis of melanocytic neoplasms.

There has been great interest in manipulating immunologic factors to treat melanomas. Clinical trials of antibodies to CTLA-4 and PD-1 have provided positive results in prolonging the life of patients with metastatic melanoma. In contrast to the advances for therapy of melanoma, there has been little progress in melanoma prevention.

Interleukin (IL)-12 and IL-23 are heterodimeric cytokines that share a common beta subunit, the IL-12p40 molecule (9). The alpha subunits, IL-12p35 and IL-23p19, provide specificity for IL-12 and IL-23, respectively (10). In animal models, IL-12 protects against development of squamous cell carcinomas of the skin and its administration reverses UVB-induced immunosuppression (11-13). These positive effects have, in large part, been attributed to its participation in the induction of Th1 and Tc1 cells that produce IFN-γ. In addition, IL-12 stimulates DNA damage repair mechanisms, and this function has been shown to play a key role in protection against UV carcinogenesis and immunosuppression (11, 12). IL-23 was described some years after the discovery of IL-12. IL-23 promotes the generation of Th17 cells that produce IL-17 and IL-22 (14). IL-23-induced DNA repair has also been reported (15).

In this study, we evaluated the role of IL-12 and IL-23 in the development of pre-malignant dysplastic nevi, melanoma and their lymph node metastases. The role of these two cytokines in cutaneous squamous cell carcinoma (SCC) development has been the focus of many investigations, but their role in melanomagenesis has not been tested. We initially hypothesized that, like 7,12-dimethylbenz(a)anthracene (DMBA)-induced SCC models, the loss of IL-23 would inhibit melanoma development. Contrary to our hypothesis, we found that IL-23 plays an important role in controlling nevus development and in inhibiting melanoma progression through direct activation of DNA repair in melanocytes, and indirectly by reducing regulatory T cell infiltration and IFNγ production.

Methods

Animals and Reagents

The study was approved by the UAB Institutional Animal Care and Use Committee. Female C3H/HeN mice aged 6-8 weeks were obtained from Charles River Breeding Laboratories (Wilmington, MA), NIH-bg-nu-xid mice 6-8 weeks old were obtained from NCI-Frederick. IL-12p35 KO and IL-12/IL-23p40 KO on a C57BL/6 background were purchased from Jackson laboratories. IL-23KO were provided by Dr. Daniel Cua (Merk Research Laboratories). IL-12p35KO, IL-12/IL-23p40KO and IL-23KO mice were backcrossed for 10-11 generations on to the C3H/HeN background by the University of Alabama at Birmingham (UAB) genetically engineered mutant mouse (GEMM) core. The C3H/HeN

character was greater than 99% as detected by 2 microsatellite markers for C3H/HeN. All animals were housed in the UAB pathogen-free animal facility, fed a normal diet, and given water ad libitum. The study was approved by the UAB Institutional Animal Care and Use Committee.

Chemicals and antibodies

7,12-dimethylbenz(a)anthracene (DMBA) (95% purity), N6, 2'-O-dibutyryladenosine 3:5-cyclic monophosphate (dbcAMP) and Sodium orthovandate (Na3VO4) were purchased from Sigma Aldrich Chemical Co. (St. Louis, MO). 12-O-tetradecanoyl-phorbol-13-acetate (TPA) was obtained from LC laboratories (Woburn, MA). Rat anti-mouse IL-12Rβ2 and IL-23R were purchased from R&D; Rabbit anti-mouse VEGF, TRP2, Mouse anti-human S100, Rat anti-mouse vimentin were obtained from Santa Cruz Biotechnology, Inc. Rat anti-mouse pERK was from BD biosciences. CD4-PE, CD4-FITC, FOXP3-PE, FOXP3-v450, IA/IE-FITC, IL-17-Percp-Cy5.5, IL-10-PE, CD45.2-Percp-Cy5.5, CD45.2-FITC were obtained from eBiosciences. IFNγ-PE-Cy7, CD8-Alexa-647, and CD8-PE were obtained from BD-pharmingen.

Carcinogenesis protocol

Mice were shaved and naired on the back skin. After a 5 day rest, they were painted with 100μg DMBA in 100μl acetone and then treated twice weekly with topical 12.5μg TPA (20nmol) (16). Before isolation of nevi or LNs, mice were rested for 5 weeks and then sacrificed (16).

Histological evaluation and melanin bleaching

Nevus biopsies or lymph nodes were processed for hematoxylin and eosin (H&E) staining (16). Corresponding sections were also melanin bleached using 0.25% potassium permanganate and 5% oxalic acid solutions and were processed for H&E or fluorescent staining (16). Images were captured with an Olympus DP70 digital camera and further analyzed using ImagePro Plus software v6.0 (Media Cybernetics, Inc., Silver Springs, MD.

DMBA-specific contact hypersensitivity (CHS) and adoptive transfer

Mice were sensitized on the abdomen with DMBA (100μl; 0.1% w/v DMBA in acetone). Elicitation of responses was assessed 5 days after sensitization by painting ears with DMBA (20 μl; 0.1% w/v DMBA in acetone) as described (17). To assess the extent of suppression by DMBA specific regulatory T cells, mice were sensitized as described above. Five days later, single cell suspensions of lymph node (LN) cells were obtained. CD4 T cells were isolated using Miltenyi beads according to the manufacturer's instructions. 10×10^6 CD4 T cells were adoptively transferred into WT mice. After 24h, mice were sensitized with DMBA. Elicitation and assessment of ear thickness was performed as described above.

Flow cytometry and fluorescence staining

Lesional tissues and adjacent skin from carcinogen treated mice or age matched untreated skin were collected for histological examination or were subjected to digestion and processing into single cell suspensions for flow cytometric staining (16).

T cell cultures and cytokine assay

For analysis of cytokines and T cell subsets during CHS, mice were sacrificed on day 3 after DMBA challenge, ear draining LNs were removed, minced with scissors and digested in HBSS containing collagenase D (1mg/ml, Roche Applied Sciences, Indianapolis, IN) and 20μg/ml DNAse I (Sigma, St. Louis) for 45 minutes. Cells were counted and 2×10^6 cells/mouse were stimulated with PMA (50ng/ml) and ionomycin (250ng/ml) for 6h in the presence of Brefeldin A (2μM) for intracellular cytokine staining. Staining profiles were obtained using a LSRII flow cytometer (BD Biosciences) and FlowJo v9.5.2 for Mac or v10.0 for Windows computers.

RNA extraction, RT-PCR and qPCR

Total RNA was extracted from individual samples using Trizol reagent (Invitrogen, Carlsbad, CA) as described elsewhere (16). Primers for *Gapdh*, *Mut-Hras*, *p16^INK4a^*, *p19^ARF^*, *Tyr*, *MelanA*, *Trp2* (16), *IL-10* (18), *IL-12p35* (19), *IL-12p40* (19), *IL-23p19* (20), *IL-17* (20), *IFNγ* (21) are described in detail elsewhere. Primers for *IL-23r* (NM_144548), *IL-12rb1* (NM_008353) and *IL-12rb2* (NM_008354) were retrieved from the primer bank (22).

Soft agar anchorage-independent growth assay

The soft agar colony-forming assay was performed as described (16, 23).

Tumorigenicity in nude mice

Cell lines cultured for no more than 5 generations were injected subcutaneously with 2×10^6 cells in PBS:matrigel (1:1) into immunocompromised mice (NIH-bg-nu-Xid). Triplicate groups of mice were injected at two sites/animal. Tumors were counted weekly and tumor volume measured using the formula for a hemiellipsoid (Volume = $1/2 \times (4\pi/3) \times (l/2) \times (w/2) \times h$, where l, length, w, width, and h, height).

Normal Melanocyte preparation, melanocytic cell lines from nevus tissue and lymph nodes (LNs)

Melanocytes were prepared using standard protocol for melanocyte isolation. Skin from 1-2 day old pups (WT or KO) was excised, washed with 70% ethanol followed by PBS. The subcutaneous tissue was dissected away and the skin sheet was incubation in dispase II (25 mg/ml, Roche Applied Science) overnight at 4°C. The epidermis was peeled off and placed in 0.05% trypsin-EDTA for 10 min at 37°C under shaking. The mixture was passed through 70 um screen and centrifuged. The pellet was washed with serum-containing media and then cells were resuspended in Opti-MEM medium containing 7% horse serum, 1% penicillin-streptomycin-glutamine, 0.05 μg/ml Fungizone, 25 ng/ml phorbol 12-myristate 13-acetate, 1 μM sodium vanadate, and 100 μM dbcAMP (all from Sigma, St. Louis, MO). The medium was changed twice weekly, and fresh phorbol 12-myristate 13-acetate was added each week. After melanocytes started to be confluent, they were divided for various experiments and used within 1-2 generations. To access their melanocytic origin, cells were stained with anti-Tyrosinase, Anti-TRP2, Anti-gp100, anti-CK14 antibodies.

Nevus tissue biopsies and LNs were digested in 200μl digestion buffer [collagenase D (Roche) (1mg/ml) and DNAse (20 μg/ml)] for 30 minutes. Cells were washed twice and then cultured in melanocyte growth medium [OptiMEM with dbcAMP (0.1mM), Na3VO4 (1μM), horse serum (7%), and phorbol 12-myristate 13-acetate (25ng/ml). Medium was changed three times a week as described (16). To access their melanocytic origin, cells were stained with anti-Tyrosinase, Anti-TRP2, Anti-gp100, anti-CK14 antibodies. For in vitro studies, the established cells lines were used within 2-3 generation. Cells were analyzed for mycoplasma using Mycoplasma detection kit (Thermo Fisher).

Statistical analysis

Data were processed by the GraphPad Prism 6.0 program (GraphPad Software for Mac). Two tailed paired Student's t-test, Two-way ANOVA, and Tukey multiple comparison tests were applied for statistical significance. Any p value <0.05 was considered significant.

Results

IL-23 prevents nevus initiation and growth

To test the influence of IL-12 and IL-23 in controlling nevus development, we treated cohorts of mice deficient in expression of IL-12p35, IL-23p19, and IL-12/IL-23p40 engineered by gene knockout (KO). Each knockout locus was backcrossed onto the nevus susceptible C3H/HeN strain for at least 10 generations. During DMBA/TPA treatment, compared to WT mice no significant differences in the latency of nevus development among the four groups, which started to appear at 6 weeks, was observed. However, in the absence of IL-23p19, an increased number and enhanced growth of nevi was observed. By 24 weeks, IL-23p19-deficient mice developed 70% more nevi, which grew 40% larger than the nevi of WT mice (**Fig. 1A-D**). To our surprise, we observed that both the number and growth of nevi were inhibited in mice deficient in IL-12p35 (p>0.05, WT versus IL-12p35KO), suggesting that IL-12 promotes pigment cell dysregulation. In the absence of both IL-12 and IL-23, an intermediate effect on initiation and growth of nevi was present, supporting the concept that the two cytokines play opposing roles in regulating melanocyte growth (**Fig. C & D**). A scatter plot of the mean size of individual nevi measured per group illustrates that loss of IL-23 has a dominant effect in promoting lesion growth, as 50% and 46% of nevi were >2 mm^2 in the double and single KO mice, respectively (p<0.001), while only ~20% of nevi reached that size in the IL-12p35KO group (**Fig. 1E-F**). Individual lesions were seen as dark spots on the skin surface and were easily discernible, even in shaded areas of hair follicle cycling (**Fig. 1G**).

To determine if nevi contained stably transformed cells or remained dependent on continuous promotion stimuli, TPA treatment was discontinued in some animals at 15 weeks and regression or growth of individual nevi was evaluated over the following 10 weeks. We observed that a subset of nevi in all groups underwent regression (**Supplementary Fig. 1A & B**). However, a greater proportion of nevi remained and continued to grow when IL-23 was absent in single or double KO mice (**Supplementary Fig. 1C**). Therefore, nevi did not depend on continued TPA treatment for autonomous growth. An IL-23p19KO mouse, left untreated for up to 8 months after treatment, developed a melanoma that had vertical growth

in addition to radial growth (**data not shown**). This was not observed for control age-matched mice treated only with TPA.

IL-23 promotes epithelial tumor development

It has been reported that IL-23 promotes DMBA/TPA-induced epithelial tumor development in C57BL/6 mice by reducing tumor-specific CD8 T cells and increasing angiogenesis (24). Therefore, we analyzed whether IL-23p19KO mice on the C3H/HeN background affected the outcome. Similar to results reported for C57BL/6 mice, C3H/HeN mice demonstrated increased resistance in IL-23p19KO mice and enhanced susceptibility in IL-12p35KO mice to development of keratinocyte-derived papillomas and squamous cell carcinomas (SCCs) (**Supplementary Fig. 1E & 1F**). The average tumor volume in IL-12p35KO and WT mice was comparable (**Supplementary Fig. 1G**). However, rather than the complete inhibition of epithelial tumors reported for IL-12/23p40KO in C57BL/6 mice (24), deficiency of both cytokines in C3H/HeN mice resulted in an intermediate number of epithelial tumors. Our results suggest that IL-23 and IL-12 have differential effects on development of epithelial versus melanocytic tumors.

IL-23 modulates the tumor microenvironment

We examined nevi by histologic and immunofluorescence staining. Lesions from all groups contained a mixture of pigmented epithelioid and spindle cells, the majority with abundant intra-cytoplasmic melanin pigment, and largely uniform nuclei (**Supplementary Fig. 2A**). Melanocyte S100 stained large areas of nevi from IL-23p19KO and IL-12/IL-23p40KO mice with a dense, bright pattern, but weakly in lesions from WT and IL-12p35KO mice (**Supplementary Fig. 2B**). Quantitative PCR specific for *MelanA* and tyrosinase (*Tyr*) mRNA confirmed that melanoma-associated gene expression was increased in lesions from IL-23p19KO and IL-12/IL-23p40KO mice compared to IL-12p35KO and WT mice (**Supplementary Fig. 2C, D**).

Since angiogenesis is a hallmark for tumor progression, we co-stained tissue sections with anti-mouse VEGF and S100 and observed that within lesions of IL-23p19KO there was elevated VEGF compared to IL-12p35KO and WT mice. This suggests that IL-23 normally inhibits angiogenesis in the melanoma tumor microenvironment (**Fig. 2A, 2B & 2C**). In addition, the proliferation marker Ki67 prominently stained S100+ cells in lesions from IL-23-deficient but not IL-12p35-deficient mice (**Fig. 2A**). In addition, an increase in tyrosinase-related protein (TRP)+ cells co-expressing the epithelial-to-mesenchymal (EMT) marker vimentin was observed in IL-23p19KO samples (**Fig. 2B**). In addition, fewer MHCII + antigen-presenting cells (**Fig. 2B**), reduced CD45.2 cells (**Fig. 2D**), and increased CD4 and CD8 cells were detected in lesions from mice deficient in IL-23p19 (**Fig. 2E**).

IL-23 reduces metastasis to lymph nodes

H&E stained sections of skin draining lymph nodes (dLNs) from IL-23p19KO and IL-12/IL-23p40KO mice contained clusters of pigmented cells, which were less evident in IL-12p35KO and WT dLNs. Benign nevus cells do occasionally accumulate in sinuses of the LN capsule and parenchyma (25), but the presence of pigmented cells in deep parenchyma can be diagnostic for melanoma metastases (26, 27) (**Fig. 3A**). Nuclear

morphology examined in pigment-bleached serial sections indicated round nuclei with prominent nucleoli, characteristic of melanocytic cells rather than pigment-laden macrophages. (**Inset Fig. 3A**). LNs from IL-23p19KO and IL-12/IL-23p40KO mice with pigmented skin lesions were laden with intense black pigmentation; this was less evident in LNs from WT and IL-12p35KO mice (**Fig. 3C**). Flow cytometric analysis of LN cells from nevus bearing mice corroborated visual assessments of LNs, where a 3-fold increase in TRP2+/MelanA+ cells was present in IL-23p19KO versus IL-12p35KO LN cells (**Fig. 3B**). Real-time qPCR also suggested higher numbers of tumor cells had invaded LNs as revealed by levels of *Trp2*, *Tyr* and *MelanA* mRNA expression (**Supplementary Fig. 3A**). To distinguish melanocytic cells from melanophages (pigment-laden macrophages), we used double immunofluorescent staining with S100 and myeloid CD11b or lymph node macrophage specific CD169 Abs. The majority of stained cells were non-overlapping distinct populations – further supporting that S100+ cells were melanocytic in origin. Interestingly, we observed more macrophage infiltration in LNs from mice deficient in IL-23p19 in contrast to LNs from WT or IL-12p35-deficient mice (**Supplementary Fig. 3B**). This finding is consistent with the known role of macrophages in establishing microenvironments that favor tumor growth (28).

IL-23 reduces prolonged survival of transformed melanocytic cells

Nevus cells can be cultured for only a limited time, and proliferate for little more than one passage before they undergo senescence (29). However, immortalized or transformed cells provide continuous cultures, and ultimately establish cell lines. Thus, we assessed the proportion of nevi, and dLNs that contained cells that could seed continuous melanocyte cultures. Lesional tissue was carefully isolated, and dLNs harvested, then processed into single cell suspensions to seed cultures. The percentage of lesions and LNs producing immortalized cell lines was significantly increased when derived from IL-23p19-deficient mice (**Fig. 3D & E**). It was very difficult to establish a cell line from LNs and lesions taken from IL-12p35-deficient mice. Further, it took 5 times more nevi to generate slow growing cell lines from IL-12p35KO mice.

Tumorigenicity is increased by IL-23-deficiency

We characterized the tumorigenic potential of cell lines derived from all groups of mice. First, their ability to grow *in vitro* as attachment-independent colonies in soft agar demonstrated that the cell lines derived from mice deficient in IL-23p19 were able to generate a greater number of colonies, which grew to a size comparable to colonies formed by the positive control melanoma line B16/F10 (**Fig. 3F**). Their tumorigenicity *in vivo* was determined by their ability to form growing tumors following subcutaneous injections into nude mice. Like the *in vitro* colony growth forming profile, cell lines from IL-23p19-deficient mice exhibited enhanced tumor-growth, with increased mitotic indices (**Fig. 3G, 3H**). In contrast, cell lines derived from WT or IL-12p35KO mice were unable to form large tumors in nude mice and contained fewer mitotic cells.

IL-23 inhibits proliferation of melanocytic cell lines

We noted that the cell lines established from the nevi of IL-23p19-deficient mice tripled their cell numbers in 2 days, while cell lines from WT or IL-12p35-deficient mice less than doubled (**Supplementary Fig. 3C**). These data are consistent with the observed increase in proliferative index by the respective tumors grown in nude mice (**Fig. 3G, 3H**). To test whether IL-23 can directly act on melanocytes and tumor cell lines, primary cultures of normal WT melanocytes and tumor cell lines were incubated in the absence or presence of rIL-23 or rIL-12 for 48h. In normal melanocytes, the number of cells doubled in cultures in which either rIL-12 or rIL-23 was present (**Supplementary Fig. 3D**), indicating that these cytokines directly stimulate normal melanocyte proliferation. However, when melanoma cultures contained rIL-23, recovery of cells was greatly reduced (approaching 50% reduction), while there was a modest inhibition (~20%) of melanoma growth in the presence of IL-12 (**Supplementary Fig. 3D**). These data suggest that IL-23 acts directly on melanocytic cells to differentially regulate the growth of normal melanocytes and melanoma.

Normal melanocytes and nevus cells express IL-12 and IL-23 receptors

To confirm that IL-12 and IL-23 can act directly on melanocytes, we analyzed expression of their receptors. We observed that normal melanocytes express both IL-12 and IL-23 receptors (**Supplementary Fig. 3E**). Interestingly, rIL-23 upregulated mRNA expression (**Supplementary Fig. 3F-G**) for both IL-23 and IL-12 receptors, while IL-12 only modestly reduced IL-12 receptor mRNA expression, but IL-12 receptor expression was low on cells. (**Supplementary Fig. 3F**). qRTPCR analysis in lesion biopsies and adjacent skin demonstrated ubiquitous IL-23 receptor expression in WT and all the cytokine KO mice. IL-12 receptor expression was lower in all three strains of KO mice compared to WT mice (**Supplementary Fig. 3H & 3I**) and this may account for our inability to detect prominent effects by rIL-12.

Robust melanocyte DNA repair is induced by IL-23

Using allele-competitive blocker (ACB) PCR, we have previously shown that nevi in this model often contain mutations in the 61st codon of the *H-ras* oncogene. Detection of that particular mutation, as well as the loss of cyclin-dependent kinase inhibitor 2a (*Cdkn2a*) gene expression (encoding p19^{Arf} and p16^{Ink4a}), which is associated with melanoma, were employed to provide readouts for the mutation burden and indirectly, the efficiency of DNA repair (**Fig. 4A**). Melanocytic cell lines established from IL-12p35 KO mice possessed fewer *H-ras* mutations compared with cell lines derived from IL-23p19 KO and WT mice (2/8 versus 5/8, respectively). Further, expression of *p19^{Arf}* and *p16^{Ink4a}* was weak or undetectable in cell lines from IL-23p19-deficient mice, compared to lines from WT or IL-12p35-deficient mice (**Fig. 4A**). Loss of *p16^{Ink4a}* expression was found at an increased frequency in nevus-derived cell lines from IL-23p19-deficient mice, supporting a role for IL-23 in maintaining DNA integrity. Therefore, we investigated whether IL-23 or IL-12 played a direct role in melanocyte DNA repair. Primary melanocytes were isolated from the skin of WT or cytokine KO mice pre-treated with DMBA. Following overnight recovery in culture, the level of nuclear DNA-damage, indicated by γH2AX red immunofluorescence, was evaluated. Thus, the absence of nuclear γH2AX stain is an indication of successful

DNA repair. DNA repair of DMBA-treated primary melanocytes from IL-12p35KO mice was augmented, while nuclei of treated melanocytes from IL-23p19KO mice remained highly positive for γH2AX, indicating poor repair of DNA (**Fig. 4B**). It should be noted that this contrasts with studies on photo-damage repair of DNA in keratinocytes (11, 15, 30). Further, the presence of rIL-23 in the culture medium promoted DNA repair (**Fig. 4C**), while neutralizing IL-23 in cultures inhibited repair (**Fig. 4D**). The modest impact of IL-12 on melanocyte DNA repair suggests that the augmented DNA repair observed for IL-12p35 KO-derived melanocytes may be due to other factors. To determine if IL-23 mRNA expression is dysregulated (i.e., increased) in IL-12p35KO melanocytes, qPCR was used. IL-23 specific p19 mRNA expression levels in IL-12p35KO and WT melanocytes were comparable. IL-23p19KO melanocytes overexpressed mRNA for the IL-12-specific p35 subunit mRNA, but mRNA for the shared IL-12 p40 subunit was reduced compared to WT and IL-12p35KO melanocytes (**Fig. 4E**). We next analyzed expression of DNA repair enzymes and observed that IL-23 induces DNA repair enzyme *Xpc* (**Fig. 4F**), while *Xpa* is induced by both IL-12 and IL-23 (data not shown).

IL-23 alters immune responses during DMBA initiation

Since IL-23 enhances DNA repair and DNA damage suppresses immune responses, we sought to determine whether there is an indirect role for IL-23p19 deficiency in the development of nevi and/or progression to melanoma. We employed allergic contact hypersensitivity (CHS) assays to measure T cell-mediated CHS responses to DMBA, the compound responsible for nevus development in this system. Recent work from our lab has shown that a significant portion of DMBA-specific T cells is raised to an epitope containing the codon 61 point mutation that activates H-ras (17). CHS responses were exaggerated in IL-12p35KO mice, but were significantly reduced in IL-23p19KO mice (**Fig. 5A**). An intermediate response was observed in IL-12/23p40KO mice, which may reflect opposing roles of IL-12 and IL-23.

CD25+CD4+Foxp3+ regulatory T cells inhibit CHS (31). In contrast to the reduced CHS response by IL-23p19KO mice, we observed that the cellularity of LNs from IL-12p35KO, IL-23p19KO and IL-12/23p40KO mice increased at least 2-fold compared to WT mice (**Fig. 5B**). Flow cytometry revealed that the percentage of CD25+CD4+Foxp3+ regulatory T cells in IL-12p35KO mice was reduced by 25% compared to WT (**Fig. 5C**). However, after adjusting for differences in cellularity, the absolute number of regulatory T cells was not significantly different from WT mice (**Fig. 5D**). IL-23p19 deficiency led to a modest increase in the percentage of CD8 T cells compared to WT or IL-12p35KO mice (**Fig. 5C**). The numbers of CD8 T cells, CD4 T cells and CD4+CD25+Foxp3 were higher in IL-23p19KO mice compared to IL-12p35KO mice (**Fig. 5D**). The CD4+, CD8+ and Foxp3+ T cells that produced IL-10 increased in CHS responding IL-23p19KO mice (**Fig. 5D, Supplementary Figure 4A-6D**), consistent with an immunosuppressive environment. This was not observed in IL-12p35KO CHS responding mice. CD4+ IFNγ or IL-17 producing cells were comparable in all groups (data not shown). On the other hand, the percentage of CD8+ IL-17 producers increased in the absence of IL-12 (i.e. IL-12p35KO and IL-12/23p40KO mice) while the absolute number of this cell subset increased in all KO mice, compared to WT mice (**Supplementary Fig. 4E&4F**). A modest but significant

increase in the percentage and absolute number of CD8+ IFNγ producers was observed in IL-23p19 and IL-12/23p40KO mice.

Since the magnitude of the CHS response is determined by the subsets of immune cells infiltrating, we next analyzed ear skin on day 3 after DMBA challenge. We observed that the absence of IL-23 enhanced infiltration of leukocytes (CD45.2 cells) into the ears of mice. Further, the percentage of CD45.2 cells that were CD4 or CD8 increased in the absence of IL-23 (**Fig. 5E**). The percentage of regulatory T cells was similar in all groups (data not shown). As expected, effector CD4+IL-17+ cells increased in IL-12p35KO mice and were reduced in IL-23p19KO and IL-12/23p40KO mice compared to WT mice, consistent with the roles for the respective cytokines in T cell subset differentiation.

The majority of CD4+IL-17+ cells were double producers of IL-17 and IFNγ (**Fig. 5E**). The CD4+IFNγ+ or CD8+IFNγ+ cell percentages were similar (**Fig. 5E**). We investigated the function of CD4+ T cells purified from DMBA sensitized WT and KO mice by testing their ability to inhibit the elicitation of CHS responses following their transfer into WT sensitized mice. We observed that CD4+ T cells from IL-12p35KO mice were unable to inhibit DMBA responses. In contrast, CD4 T cells from IL-23p19KO mice contained functional regulatory T cells that profoundly inhibited responses (**Fig. 5F**). We assessed the contribution of CD4 T cells for nevus development and addressed whether IL-23 was important for elaborating the CD4-dependent mechanism by examining nevus development in single and double KOs for CD4 and IL-23p19 (**Fig. 5G**). Without CD4 T cells only a few nevi developed, which were small in size compared to nevi in WT mice. With IL-23p19KO mice we reproduced the finding that appreciably more and significantly larger nevi were generated. However, mice deficient in both IL-23p19 and CD4 generated an intermediate number of lesions, falling between the numbers generated by the single knockout mice. This result suggests IL-23 mediated control of melanocyte dysregulation is operated by both T cell dependent and independent mechanisms (e.g., DNA repair). Double KO mice for CD8 and IL-23 were similar to single IL-23p19KO with respect to nevus development, indicating CD8 T cells may not be involved in IL-23 mediated nevus inhibition (**Supplementary Fig. 4G & 4H**). In IL-12p35-CD8 double KO mice, we observed increased numbers of nevi and an increase in average lesion size compared to IL-12p35KO, indicating IL-12 alters CD8 function (**Supplementary Fig. 4I & 4J**).

IL-23 blocks tumor promoting IFNγ

Since IFNγ has been implicated in melanomagenesis (32), we next investigated whether IFNγ levels were increased in the absence of IL-23 (**Fig. 6A**), qRT-PCR analysis of skin mRNA, isolated 24 hours after TPA treatment, revealed IFNγ mRNA levels that were dramatically elevated in the absence of IL-23, but not in the absence of IL-12. Not surprisingly, the absence of IL-23 reduced IL-17 mRNA expression in both the single and double KO specimens (**Fig. 6B**). However, in the absence of IL-12, a modest increase in IL-17 mRNA was observed. Intriguingly, a four-fold increase in IL-10 mRNA expression was observed in TPA treated IL-23p19KO skin (**Fig. 6C**). The respective roles for IFNγ and IL-17 in nevus formation were tested by infusion of neutralizing antibody in WT mice during carcinogenesis. We observe that injection of anti-IFNγ but not anti-IL-17 antibody

resulted in a reduction in nevus numbers and size, supporting a pro-tumorigenic role of IFNγ for nevus development (**Fig. 6D-G**).

Discussion

Basic research and clinical observations over the past several decades have clearly demonstrated that immunological mechanisms are capable of controlling melanoma growth and development. This line of investigation has led to the introduction of novel immunotherapeutic agents that prolong the survival of patients with advanced melanomas. Most melanomas begin as premalignant dysplastic nevi, which after months to years, may progress to become invasive melanomas. Thus, there is ample opportunity to prevent dysplastic nevi from evolving into melanomas. Identification of novel agents that can avert melanoma development has proceeded slowly, at least in part because of the limited number of preclinical models that can be used to evaluate potential protective modalities. This is particularly true for immunological interventions. Existing mouse melanoma models are largely restricted to transplantable syngeneic melanoma lines, such as B16, compatible only with C57BL/6 mice, or transgenic mice with enforced expression of mutant oncogenes. These animal models rapidly develop melanomas without first showing evidence of dysplastic nevi.

To address these gaps in our knowledge, we created an in vivo model in which mice develop large numbers of pigmented nevi that progress to become invasive melanomas and then metastasize to regional lymph nodes (16). The clinical, genetic and biochemical features closely resemble those that occur in humans. We employed this model to investigate the role that IL-23 plays in melanoma development. Based on its effect in the development of chemically-induced cutaneous tumors of epithelial origin, we postulated that IL-23 would augment melanoma development in our model system, and that IL-12 would have the opposite effect. In fact, we found exactly the opposite; IL-23p19-deficient mice had more numerous nevi that grew more rapidly, resulting in larger melanocytic neoplasms that were more likely to metastasize. In contrast, IL-12p35 deficient mice, developed fewer melanocytic tumors than wild type mice.

Figure 7 summarises our finding on how IL-23 affects melanoma and SCC tumor development. Our observations of the anti-tumor effects of IL-23 in melanoma are consistent with that of others in different tumor systems. For example, IL-23 has anti-neoplastic effects when expressed as a transgene in various tumor cell vaccine models (14, 33). Further, rIL-23 can directly inhibit the proliferation of lung cancer cells in culture (34).

In contrast to the findings in our model of melanoma, there are many studies to support the concept that IL-23 promotes, rather than retards, the growth of certain types of tumors (24, 35). For example, Langowski *et al.*, reported that IL-23 was important for promoting the development of epithelial squamous cell carcinoma (SCC) induced by chemical carcinogenesis in mice (24). Mechanisms of tumor promotion were linked with IL-23-associated tumor angiogenesis and inhibition of tumor-infiltrating CD8 T cells (24). Further, our previous results have shown that IL-17 producing Th17 cells promote SCC development in DMBA/TPA treated mice (36-38). Our data confirm those studies with respect to

squamous cell carcinomas of the skin (see Supplementary Figure 2). The conflicting literature indicates that the mechanisms relating to IL-23-mediated direct and/or indirect effects on tumorigenesis remain obscure and confusing (14). The pro- or anti-tumorigenic activity of these cytokines may be affected by a number of factors, including the tumor type, the type of induced damage, tissue specific responses, and differences in the concentrations of IL-12 and IL-23 cytokines in the microenvironment.

Our findings in this system provide convincing evidence that IL-23 and IL-12 produce different effects depending on the cell type. Melanocytic lesions and keratinocyte-derived papillomas exhibited a reciprocal relationship. Tumor development was evaluated in the same mice and in the same treatment area and all of the other conditions were the same. More melanomas and fewer SCCs were observed in the IL-23p19 deficient mice; more SCCs and fewer melanomas were found in the IL-12p35-deficient mice. One explanation for this may be differences in IL-12 and IL-23 receptor expression or response between the two cell types. We were able to demonstrate that melanocytic cells expressed receptors for IL-23 and those receptors enhanced DNA repair processes in that cell type. In contrast to the studies in which DMBA was the initiating agent, studies investigating UV-radiation-induced epithelial tumor development support an inhibitory role for IL-23. Tumor incidence increased in IL-23p19-deficient mice whereas the loss of IL-12 had no effect (39). Further work showed that like IL-12, IL-23 induced DNA repair following photo-damage, and this activity was proposed to contribute to its anti-tumorigenic function (15). Thus, the initial carcinogenic stimulus also determines the pro- or anti-carcinogenic effect of IL-12 and IL-23.

There is some evidence in humans suggesting that IL-23 also plays a role in nevus development. IL-23 plays a pivotal role in the pathogenesis of psoriasis (40) and one study (41) describes patients with psoriasis who showed a reduction in nevus numbers in the psoriatic lesions. Another study (42) observed that compared with control subjects, psoriatic patients had fewer nevi overall, fewer nevi less than 5 mm, and fewer congenital nevi. The use of biologics in the patients was a risk factor for a higher nevus count, whereas disease severity did not correlate with number of nevi. Our study provides additional evidence that IL-23 contributes to nevus development. The data imply that care may need to be taken when treating autoimmune diseases with IL-23 neutralizing antibodies.

As was mentioned, IL-23 was found to directly block tumor initiation and growth through augmentation in DNA repair. IL-23 not only acted at this stage of tumorigenesis, it also inhibited regulatory T cell expansion, and in so doing, diminished IFNγ responses in the skin. IFNγ is a double edged cytokine that acts both as an anti-tumor and a pro-tumorigenic cytokine. Anti-tumor mechanisms of IFNγ are well understood. IFNγ inhibits cell-meditated immune responses through generation of regulatory T cells (43).

Pro-tumor characteristics of IFNγ are also described (44). A melanoma-promoting role for IFNγ has been reported by Zaidi *et al*. Their study employed neonatal UV irradiation in mice, and identified IFNγ producing macrophages during initiation, which played a key role in making competent melanoma precursors in mice and humans (32). Neutrophils also secrete IFNγ in response to stimulation (45). We observed that the loss of IL-12 reduced

IL-12-dependent IFNγ+ T cells. In addition, IFNγ production from activated NK, Th1 and CD8 T cells may also play an important role in promoting melanoma. IFNγ receptors are present on melanocytes, and work by others report that IFNγ can inhibit apoptosis of UVR damaged melanocytes (46), thus promoting tumor development. Further, IFNγ induces iNOS in melanocytes (47), which is an important anti-apoptotic and pro-inflammatory protein (48). IL-23 can also activate gamma delta T cells and NK cells (49, 50). Both cell types are known to inhibit melanoma development (51). The precise nature of IL-23 mediated mechanisms that maintain melanocyte homeostasis still needs to be addressed in future investigations. Thus, this study is first to elucidate the importance of IL-23 in controlling melanomagenesis and indicates that care must be taken when considering anti-cytokine therapies for treating patients that may have increased susceptibility to melanoma.

Supplementary Material

Refer to Web version on PubMed Central for supplementary material.

Acknowledgments

References

1. Siegel R, Ma J, Zou Z, Jemal A. Cancer statistics, 2014. CA: a cancer journal for clinicians. 2014; 64:9–29. [PubMed: 24399786]

2. Gandini S, Autier P, Boniol M. Reviews on sun exposure and artificial light and melanoma. Progress in biophysics and molecular biology. 2011; 107:362–366. [PubMed: 21958910]

3. Greene MH, Clark WH Jr. Tucker MA, Kraemer KH, Elder DE, Fraser MC. High risk of malignant melanoma in melanoma-prone families with dysplastic nevi. Annals of internal medicine. 1985; 102:458–465. [PubMed: 3977193]

4. Goldstein AM, Chan M, Harland M, Hayward NK, Demenais F, Bishop DT, Azizi E, Bergman W, Bianchi-Scarra G, Bruno W, Calista D, Albright LA, Chaudru V, Chompret A, Cuellar F, Elder DE, Ghiorzo P, Gillanders EM, Gruis NA, Hansson J, Hogg D, Holland EA, Kanetsky PA, Kefford RF, Landi MT, Lang J, Leachman SA, MacKie RM, Magnusson V, Mann GJ, Bishop JN, Palmer JM, Puig S, Puig-Butille JA, Stark M, Tsao H, Tucker MA, Whitaker L, Yakobson E. Features associated with germline CDKN2A mutations: a GenoMEL study of melanoma-prone families from three continents. Journal of medical genetics. 2007; 44:99–106. [PubMed: 16905682]

5. Goldstein AM, Chan M, Harland M, Hayward NK, Demenais F, Bishop DT, Azizi E, Bergman W, Bianchi-Scarra G, Bruno W, Calista D, Albright LA, Chaudru V, Chompret A, Cuellar F, Elder DE, Ghiorzo P, Gillanders EM, Gruis NA, Hansson J, Hogg D, Holland EA, Kanetsky PA, Kefford RF, Landi MT, Lang J, Leachman SA, MacKie RM, Magnusson V, Mann GJ, Bishop JN, Palmer JM, Puig S, Puig-Butille JA, Stark M, Tsao H, Tucker MA, Whitaker L, Yakobson E, Lund Melanoma Study G, Melanoma Genetics C. Features associated with germline CDKN2A mutations: a GenoMEL study of melanoma-prone families from three continents. Journal of medical genetics. 2007; 44:99–106. [PubMed: 16905682]

6. Goldstein AM, Fraser MC, Struewing JP, Hussussian CJ, Ranade K, Zametkin DP, Fontaine LS, Organic SM, Dracopoli NC, Clark WH Jr. et al. Increased risk of pancreatic cancer in melanoma-prone kindreds with p16INK4 mutations. The New England journal of medicine. 1995; 333:970–974. [PubMed: 7666916]

7. Eskandarpour M, Hashemi J, Kanter L, Ringborg U, Platz A, Hansson J. Frequency of UV-inducible NRAS mutations in melanomas of patients with germline CDKN2A mutations. J Natl Cancer I. 2003; 95:790–798.

8. Papp T, Pemsel H, Zimmermann R, Bastrop R, Weiss DG, Schiffmann D. Mutational analysis of the N-ras, p53, p16INK4a, CDK4, and MC1R genes in human congenital melanocytic naevi. J Med Genetics. 1999; 36:610–614. [PubMed: 10465111]

9. Hunter CA. New IL-12-family members: IL-23 and IL-27, cytokines with divergent functions. Nat Rev Immunol. 2005; 5:521–531. [PubMed: 15999093]

10. Trinchieri G. Immunobiology of interleukin-12. Immunol Res. 1998; 17:269–278. [PubMed: 9479588]

11. Schwarz A, Stander S, Berneburg M, Bohm M, Kulms D, van Steeg H, Grosse-Heitmeyer K, Krutmann J, Schwarz T. Interleukin-12 suppresses ultraviolet radiation-induced apoptosis by inducing DNA repair. Nature cell biology. 2002; 4:26–31. [PubMed: 11780128]

12. Schwarz A, Grabbe S, Aragane Y, Sandkuhl K, Riemann H, Luger TA, Kubin M, Trinchieri G, Schwarz T. Interleukin-12 prevents ultraviolet B-induced local immunosuppression and overcomes UVB-induced tolerance. J Invest Dermatol. 1996; 106:1187–1191. [PubMed: 8752655]

13. Meeran SM, Mantena SK, Elmets CA, Katiyar SK. (−)-Epigallocatechin-3-gallate prevents photocarcinogenesis in mice through interieukin-12-dependent DNA repair. Cancer research. 2006; 66:5512–5520. [PubMed: 16707481]

14. Ngiow SF, Teng MW, Smyth MJ. A balance of interleukin-12 and -23 in cancer. Trends Immunol. 2013; 34:548–555. [PubMed: 23954142]

15. Majewski S, Jantschitsch C, Maeda A, Schwarz T, Schwarz A. IL-23 antagonizes UVR-induced immunosuppression through two mechanisms: reduction of UVR-induced DNA damage and inhibition of UVR-induced regulatory T cells. The Journal of investigative dermatology. 2010; 130:554–562. [PubMed: 19727119]

16. Nasti TH, Cochran JB, Tsuruta Y, Yusuf N, McKay K, Athar M, Timares L, E. C.A. A Murine Model for the Development of Melanocytic Nevi and their Progression to Melanoma. Molecular carcinogenesis. 2016; 55:646–658. [PubMed: 25788145]

17. Nasti TH, Rudemiller KJ, Cochran JB, Kim HK, Tsuruta Y, Fineberg NS, Athar M, Elmets CA, Timares L. Immunoprevention of chemical carcinogenesis through early recognition of oncogene mutations. Journal of immunology. 2015; 194:2683–2695.

18. Fontenot JD, Gavin MA, Rudensky AY. Foxp3 programs the development and function of CD4+CD25+ regulatory T cells. Nature immunology. 2003; 4:330–336. [PubMed: 12612578]

19. Kocieda VP, Adhikary S, Emig F, Yen JH, Toscano MG, Ganea D. Prostaglandin E2-induced IL-23p19 subunit is regulated by cAMP-responsive element-binding protein and C/AATT enhancer-binding protein beta in bone marrow-derived dendritic cells. The Journal of biological chemistry. 2012; 287:36922–36935. [PubMed: 22977257]

20. Grivennikov SI, Wang K, Mucida D, Stewart CA, Schnabl B, Jauch D, Taniguchi K, Yu GY, Osterreicher CH, Hung KE, Datz C, Feng Y, Fearon ER, Oukka M, Tessarollo L, Coppola V, Yarovinsky F, Cheroutre H, Eckmann L, Trinchieri G, Karin M. Adenoma-linked barrier defects and microbial products drive IL-23/IL-17-mediated tumour growth. Nature. 2012; 491:254–258. [PubMed: 23034650]

21. Wang C, Xiao M, Liu X, Ni C, Liu J, Erben U, Qin Z. IFN-gamma-mediated downregulation of LXA4 is necessary for the maintenance of nonresolving inflammation and papilloma persistence. Cancer research. 2013; 73:1742–1751. [PubMed: 23319805]

22. Wang X, Seed B. A PCR primer bank for quantitative gene expression analysis. Nucleic acids research. 2003; 31:e154. [PubMed: 14654707]

23. Greulich H, Chen TH, Feng W, Janne PA, Alvarez JV, Zappaterra M, Bulmer SE, Frank DA, Hahn WC, Sellers WR, Meyerson M. Oncogenic transformation by inhibitor-sensitive and -resistant EGFR mutants. PLoS Med. 2005; 2:e313. [PubMed: 16187797]

24. Langowski JL, Zhang X, Wu L, Mattson JD, Chen T, Smith K, Basham B, McClanahan T, Kastelein RA, Oft M. IL-23 promotes tumour incidence and growth. Nature. 2006; 442:461–465. [PubMed: 16688182]

25. Patterson JW. Nevus cell aggregates in lymph nodes. Am J Clin Pathol. 2004; 121:13–15. [PubMed: 14750235]

26. Mentrikoski MJ, Ma L, Pryor JG, McMahon LA, Yang Q, Spaulding BO, Scott GA, Wang HL, Xu H. Diagnostic utility of IMP3 in segregating metastatic melanoma from benign nevi in lymph nodes. Modern pathology : an official journal of the United States and Canadian Academy of Pathology, Inc. 2009; 22:1582–1587.

27. Prieto VG. Sentinel lymph nodes in cutaneous melanoma. Clinics in laboratory medicine. 2011; 31:301–310. [PubMed: 21549243]

28. Ribatti D, Nico B, Crivellato E, Vacca A. Macrophages and tumor angiogenesis. Leukemia. 2007; 21:2085–2089. [PubMed: 17878921]

29. Lavado A, Matheu A, Serrano M, Montoliu L. A strategy to study tyrosinase transgenes in mouse melanocytes. BMC Cell Biol. 2005; 6:18. [PubMed: 15826307]

30. Katiyar SK, Mantena SK, Meeran SM, Elmets CA. (−)-Epigallocatechin-3-gallate from green tea prevents photocarcinogenesis in mice through augmentation of repair of UV-damaged DNA via interleukin-12-dependent mechanisms. Journal of Investigative Dermatology. 2006; 126:132–132.

31. Yusuf N, Nasti TH, Katiyar SK, Jacobs MK, Seibert MD, Ginsburg AC, Timares L, Xu H, Elmets CA. Antagonistic roles of CD4(+) and CD8(+) T-cells in 7,12-dimethylbenz(a)anthracene cutaneous carcinogenesis. Cancer Research. 2008; 68:3924–3930. [PubMed: 18483278]

32. Zaidi MR, Davis S, Noonan FP, Graff-Cherry C, Hawley TS, Walker RL, Feigenbaum L, Fuchs E, Lyakh L, Young HA, Hornyak TJ, Arnheiter H, Trinchieri G, Meltzer PS, De Fabo EC, Merlino G. Interferon-gamma links ultraviolet radiation to melanomagenesis in mice. Nature. 2011; 469:548–553. [PubMed: 21248750]

33. Lo CH, Lee SC, Wu PY, Pan WY, Su J, Cheng CW, Roffler SR, Chiang BL, Lee CN, Wu CW, Tao MH. Antitumor and antimetastatic activity of IL-23. Journal of immunology. 2003; 171:600–607.

34. Li J, Zhang L, Zhang J, Wei Y, Li K, Huang L, Zhang S, Gao B, Wang X, Lin P. Interleukin 23 regulates proliferation of lung cancer cells in a concentration-dependent way in association with the interleukin-23 receptor. Carcinogenesis. 2013; 34:658–666. [PubMed: 23250909]

35. Langowski JL, Kastelein RA, Oft M. Swords into plowshares: IL-23 repurposes tumor immune surveillance. Trends Immunol. 2007; 28:207–212. [PubMed: 17395538]

36. Yusuf N, Katiyar SK, Elmets CA. The immunosuppressive effects of phthalocyanine photodynamic therapy in mice are mediated by CD4+ and CD8+ T cells and can be adoptively transferred to naive recipients. Photochemistry and photobiology. 2008; 84:366–370. [PubMed: 18208456]

37. He D, Li H, Yusuf N, Elmets CA, Li J, Mountz JD, Xu H. IL-17 Promotes Tumor Development through the Induction of Tumor Promoting Microenvironments at Tumor Sites and Myeloid-Derived Suppressor Cells. Journal of immunology. 2010; 184:2281–2288.

38. He D, Li H, Yusuf N, Elmets CA, Athar M, Katiyar SK, Xu H. IL-17 mediated inflammation promotes tumor growth and progression in the skin. PloS one. 2012; 7:e32126. [PubMed: 22359662]

39. Jantschitsch C, Weichenthal M, Proksch E, Schwarz T, Schwarz A. IL-12 and IL-23 affect photocarcinogenesis differently. The Journal of investigative dermatology. 2012; 132:1479–1486. [PubMed: 22297634]

40. Kim J, Krueger JG. Highly Effective New Treatments for Psoriasis Target the IL-23/Type 17 T Cell Autoimmune Axis. Annual review of medicine. 2016

41. Bonifazi E. Nevus spilus appearing at birth as multiple congenital melanocytic nevi. Eur. J. Pediat. Dermatol. 2013; 23:52–53.

42. Di Cesare A, Riitano A, Suppa M, Fidanza R, Zangrilli A, Esposito M, Fargnoli MC, Chimenti S, Peris K. Frequency of melanocytic nevi in psoriatic patients is related to treatment and not to disease severity. Journal of the American Academy of Dermatology. 2013; 69:947–953. [PubMed: 24094540]

43. Kelchtermans H, Billiau A, Matthys P. How interferon-gamma keeps autoimmune diseases in check. Trends Immunol. 2008; 29:479–486. [PubMed: 18775671]

44. Xiao M, Wang C, Zhang J, Li Z, Zhao X, Qin Z. IFNgamma promotes papilloma development by up-regulating Th17-associated inflammation. Cancer research. 2009; 69:2010–2017. [PubMed: 19244111]

45. Sturge CR, Benson A, Raetz M, Wilhelm CL, Mirpuri J, Vitetta ES, Yarovinsky F. TLR-independent neutrophil-derived IFN-gamma is important for host resistance to intracellular pathogens. Proceedings of the National Academy of Sciences of the United States of America. 2013; 110:10711–10716. [PubMed: 23754402]

46. Coleman DJ, Garcia G, Hyter S, Jang HS, Chagani S, Liang X, Larue L, Ganguli-Indra G, Indra AK. Retinoid-X-receptors (alpha/beta) in melanocytes modulate innate immune responses and differentially regulate cell survival following UV irradiation. PLoS genetics. 2014; 10:e1004321. [PubMed: 24810760]

47. Fecker LF, Eberle J, Orfanos CE, Geilen CC. Inducible nitric oxide synthase is expressed in normal human melanocytes but not in melanoma cells in response to tumor necrosis factor-alpha, interferon-gamma, and lipopolysaccharide. The Journal of investigative dermatology. 2002; 118:1019–1025. [PubMed: 12060397]

48. Salvucci O, Yao L, Villalba S, Sajewicz A, Pittaluga S, Tosato G. Regulation of endothelial cell branching morphogenesis by endogenous chemokine stromal-derived factor-1. Blood. 2002; 99:2703–2711. [PubMed: 11929756]

49. Sutton CE, Lalor SJ, Sweeney CM, Brereton CF, Lavelle EC, Mills KH. Interleukin-1 and IL-23 induce innate IL-17 production from gammadelta T cells, amplifying Th17 responses and autoimmunity. Immunity. 2009; 31:331–341. [PubMed: 19682929]

50. van de Wetering D, de Paus RA, van Dissel JT, van de Vosse E. IL-23 modulates CD56+/CD3− NK cell and CD56+/CD3+ NK-like T cell function differentially from IL-12. International immunology. 2009; 21:145–153. [PubMed: 19088061]

51. Lozupone F, Pende D, Burgio VL, Castelli C, Spada M, Venditti M, Luciani F, Lugini L, Federici C, Ramoni C, Rivoltini L, Parmiani G, Belardelli F, Rivera P, Marcenaro S, Moretta L, Fais S. Effect of human natural killer and gammadelta T cells on the growth of human autologous melanoma xenografts in SCID mice. Cancer research. 2004; 64:378–385. [PubMed: 14729648]
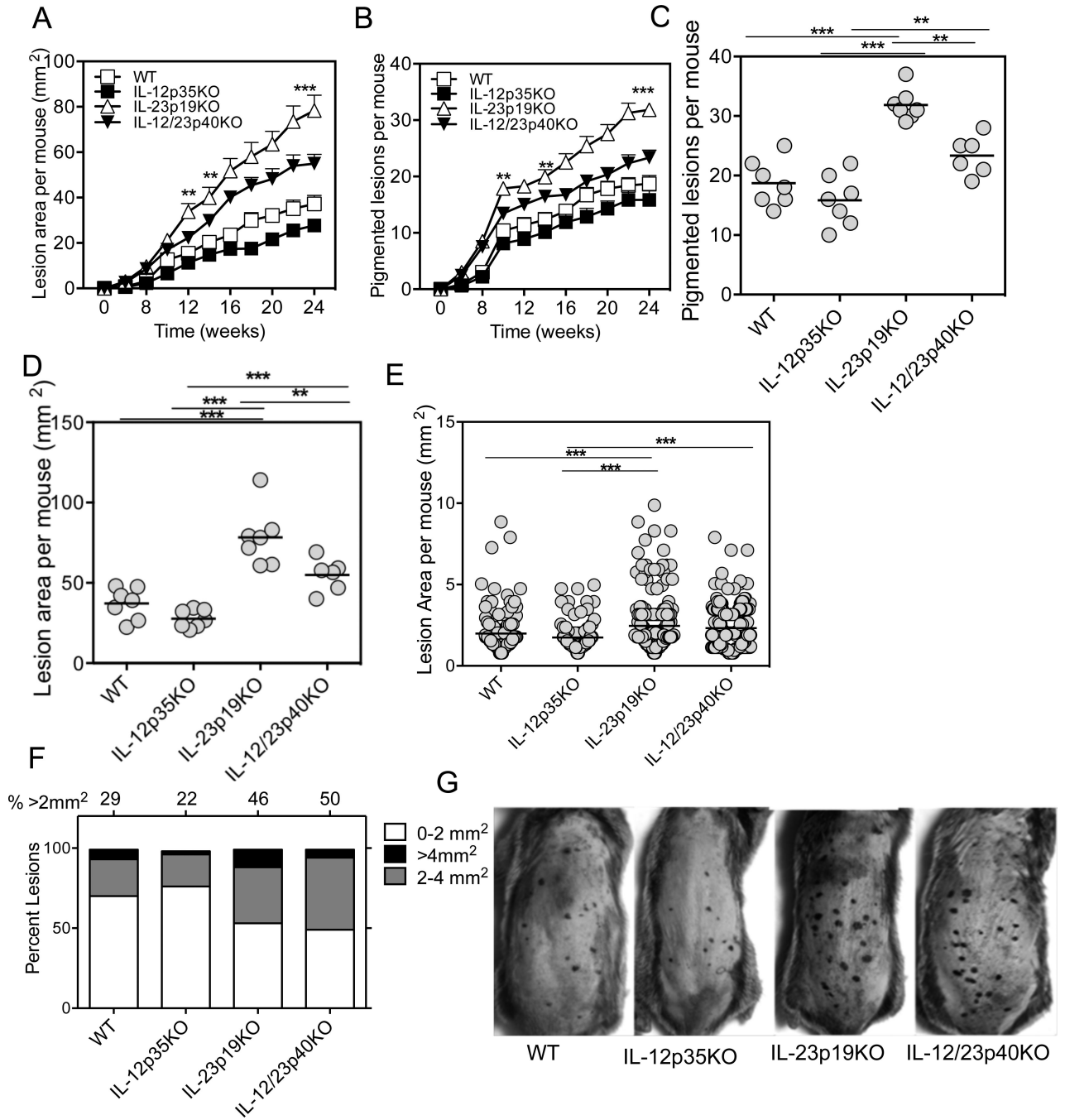
Figure 1. IL-23 inhibits the incidence and growth of pigmented lesions
DMBA (100 μg/mouse) was applied on the shaved and naired backs of mice and one week later TPA (12.5 μg/mouse) was applied twice weekly for 24 weeks. Lesions were counted and area measured twice weekly. **(A)** IL-23p19KO lesions were significantly greater in numbers compared with WT, IL-12p35KO, IL-12/23p40KO mice. **(B)** Increased lesion area per mouse in IL-23p19KO mice but not in IL-12p35KO or WT mice. Similar to the lesion number, the lesion area was significantly increased in IL-23p19KO and IL-12/23p40KO mice compared to WT and IL-12p35KO mice. Week 24 representation of nevus numbers **(C)**

and mean nevus area **(D)** per mouse among the groups described above. **(E)** Lesion area of each individual lesion at Week 24 for each group. In both IL-23p19KO and IL-12/23p40KO mice average lesion area is larger than the area of lesion from both IL-12p35KO and WT mice (p<0.001). **(F)** Stacked bar graph for lesion area at week 24 from each group, shows that in both IL-23p19KO and IL-12/23p40KO mice there is an increased percentage of lesions larger than 2 mm^2 or 4 mm^2 as compared to WT or IL-12p35KO mice. **(G)** Representative photos of mice at 15 weeks after DMBA application. Note that individual lesions are identified as darkened spots on the skin surface and are easily discernible, even in darkened areas of hair follicle cycling. ** is p<0.01. ***is p<0.001. Data is representation of one experiment from two independent experiments (n=7-10 mice).
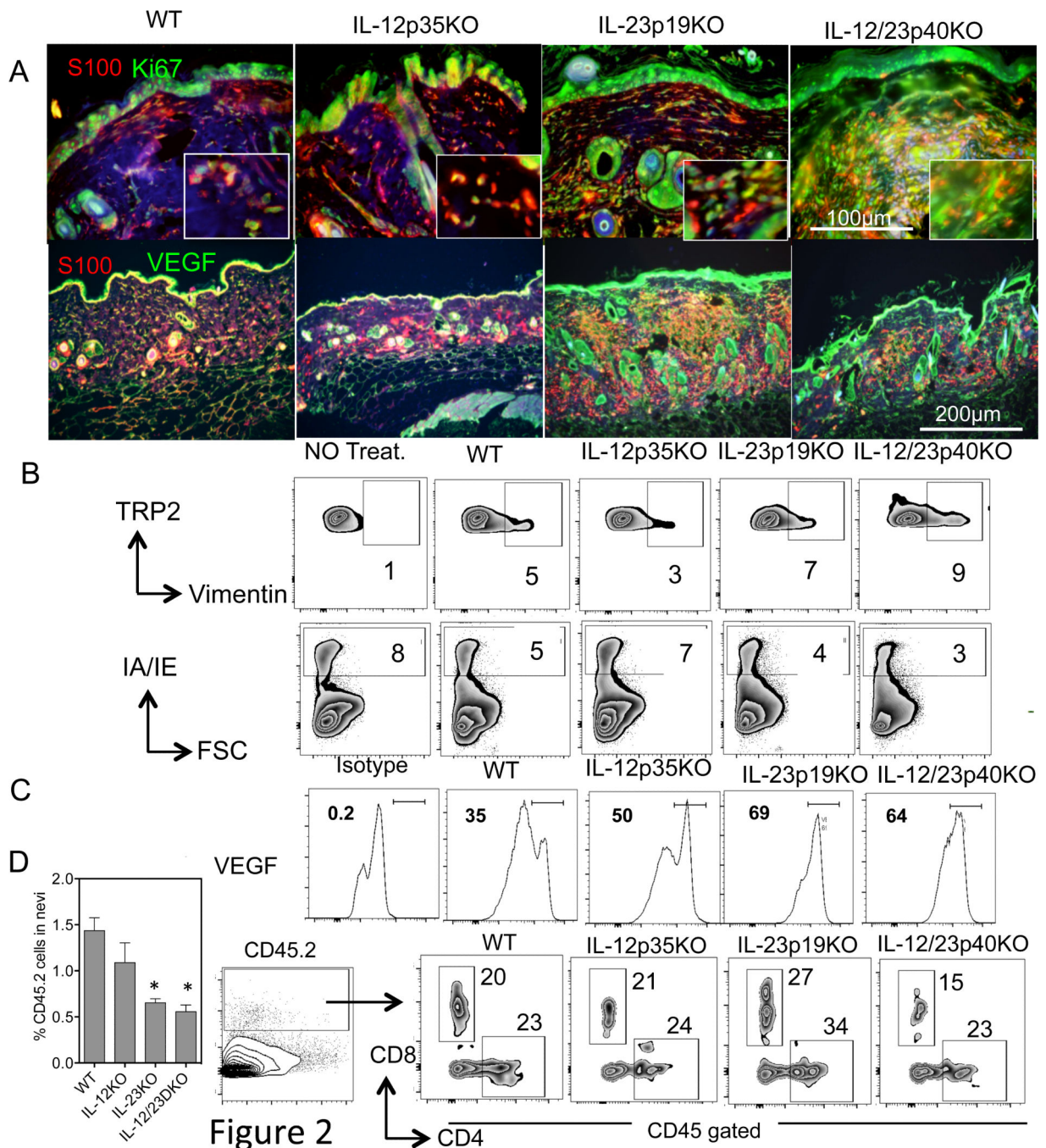
Figure 2. IL-23 inhibits angiogenic and survival signals in nevus cells

(**A**) Tissues were fixed in 10% formalin overnight and paraffin embedded tissues were cut (4-6 μm). The slides were deparaffinized and bleached to remove melanin as described in the Materials and Methods. The sections were stained with anti-mouse S100 antibody [clone 4C4.9] (red) and rabbit anti-mouse VEGF (clone A-20) (Green) or rabbit anti-mouse Ki67 (Green). All the slides were incubated with DyLight 594 donkey anti-mouse IgG or DyLight 594 donkey anti-rabbit IgG. After the final wash all sections were counterstained with DAPI to stain nuclei. The pictures were taken with a 20x objective lens. The red intensity in WT

and IL-12KO lesions was increased to make the nevus area distinguishable. Two mice from each group were sacrificed and nevus tissue isolated and treated as discussed in the Materials and Methods section. The single cell suspensions were counted and stained for FACS analysis. The cells were gated on the melanocytic marker anti-mouse TRP-2. These cells were then analyzed for **(B)** Vimentin, MHCII and **(C)** VEGF. **(D)** Percent CD45.2 cells in nevi of KO mice. Single cell suspension were stained with anti-CD45.2, CD4 and CD8 antibody and analyzed by flow cytometry. The cells were gated on CD45.2 and then analyzed for CD4 and CD8 staining as shown. For microscopy, 3-5 nevi were stained. Data is representation of one nevi from one of the experiments. For flow 3-5 nevi were pooled from 5 different mice. * is p<0.05.
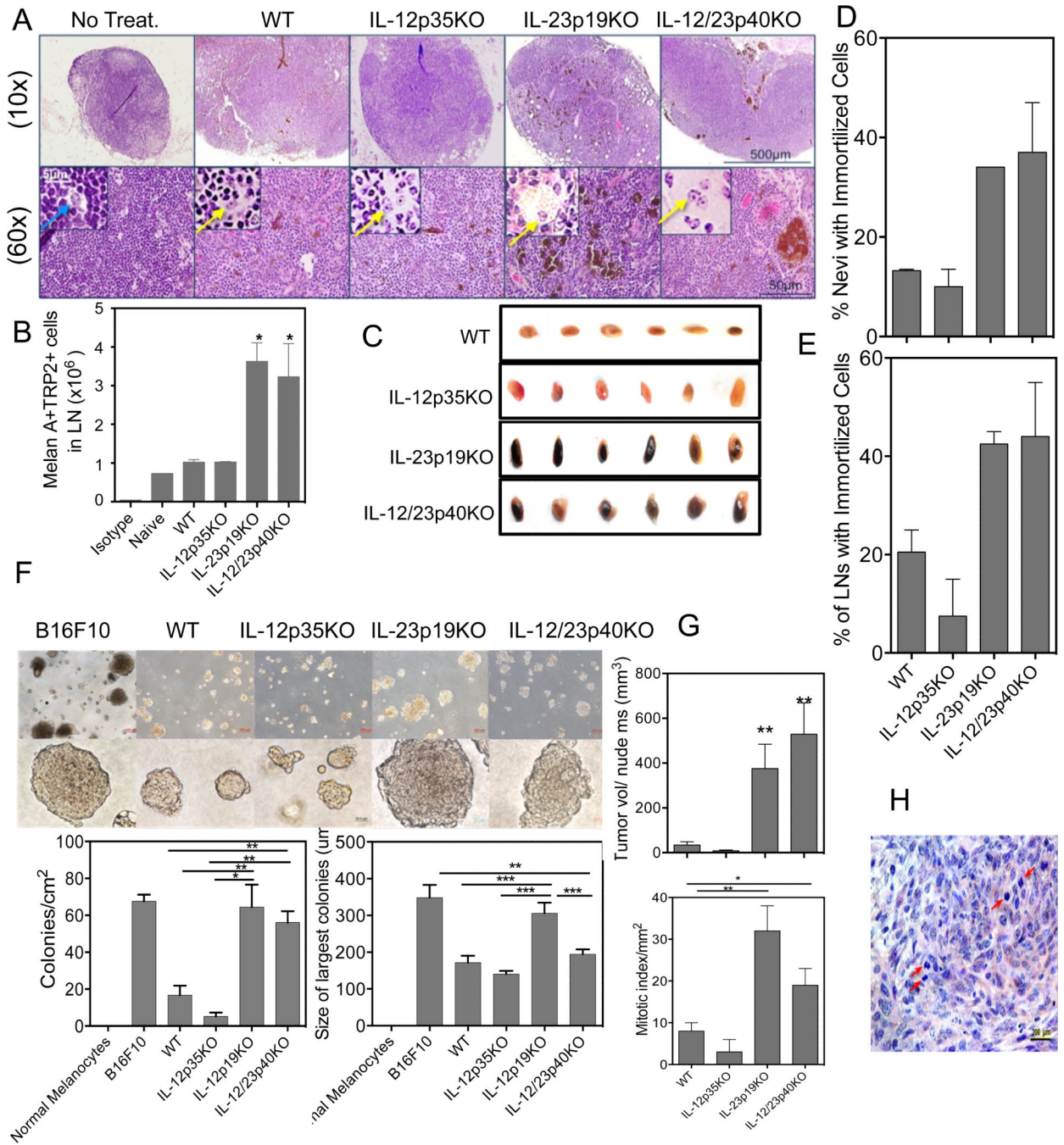
Figure 3. IL-23 inhibits metastasis and prolonged survival of pigmented cells

(A) Histologic evidence of migratory pigment cells in LNs. Panels of H&E stained lymph node serial section pairings of unbleached and bleached (inset) views taken with objective magnification of 10x or 60x as shown. Patterns differed in enhanced infiltration of pigmented tumor cells throughout the IL-12p35KO and IL-23p19KO mice lymph nodes while only a few small islands of pigmented tumor cells were present in IL-12p35KO and WT mice lymph nodes. Age matched normal mice (No Treatment control) contained minimal numbers of pigmented cells, identified by nuclear morphology (blue arrow). Insets

highlight nuclei with open chromatin and prominent nucleoli (yellow arrows). (B) Increased melanoma marker positive cells in LN of IL-23KO mice. LN single cell suspensions (2×10^6) were stained with anti-mouse Trp2 and anti-mouse Melan A antibody, then with the appropriate secondary antibody for analysis by flow cytometry. The numbers are pooled data from 4 lymph nodes of two mice from two different experiments. **(C)** The visual representation of lymph nodes from all the groups of mice. These are two lymph nodes each from three different mice in each group. **(D & E)** Percent nevi and LNs per group that produced an immortalized cell line. Control skin of each mouse strain, treated only with TPA, were unable to produce a cell line. This is the mean of 2 experiments with at least 10 nevi or LNs in each group. **(F)** Nevus cells derived from the IL-23p19KO grew robustly in soft agar, and supported high numbers of colony forming cells, capable of forming large colonies, with characteristics that were indistinguishable from B16F10 melanoma, a highly aggressive murine melanoma tumor line. In contrast, the IL-12 p35 deficient lesion cells demonstrated poorer growth in soft agar, producing significantly fewer colonies that were also smaller in size and were comparable to WT colonies. **(G)** Cell lines derived from lesions were injected in nude mice at 1×10^6 per mouse in triplicate. (H) Increased mitotic index of tumors formed by IL-23p19 KO-derived nevus lines. Mitotic figures were counted from 10 fields of duplicate tumors, stained by H&E (example shown in bottom panel) and read blind by a dermatopathologist. Arrows highlight mitotic figures. *p is <0.05. ** is p<0.01. ***is p<0.001. Data is representation of one of the two independent experiments. For growth in nude mice (n=3) were used.
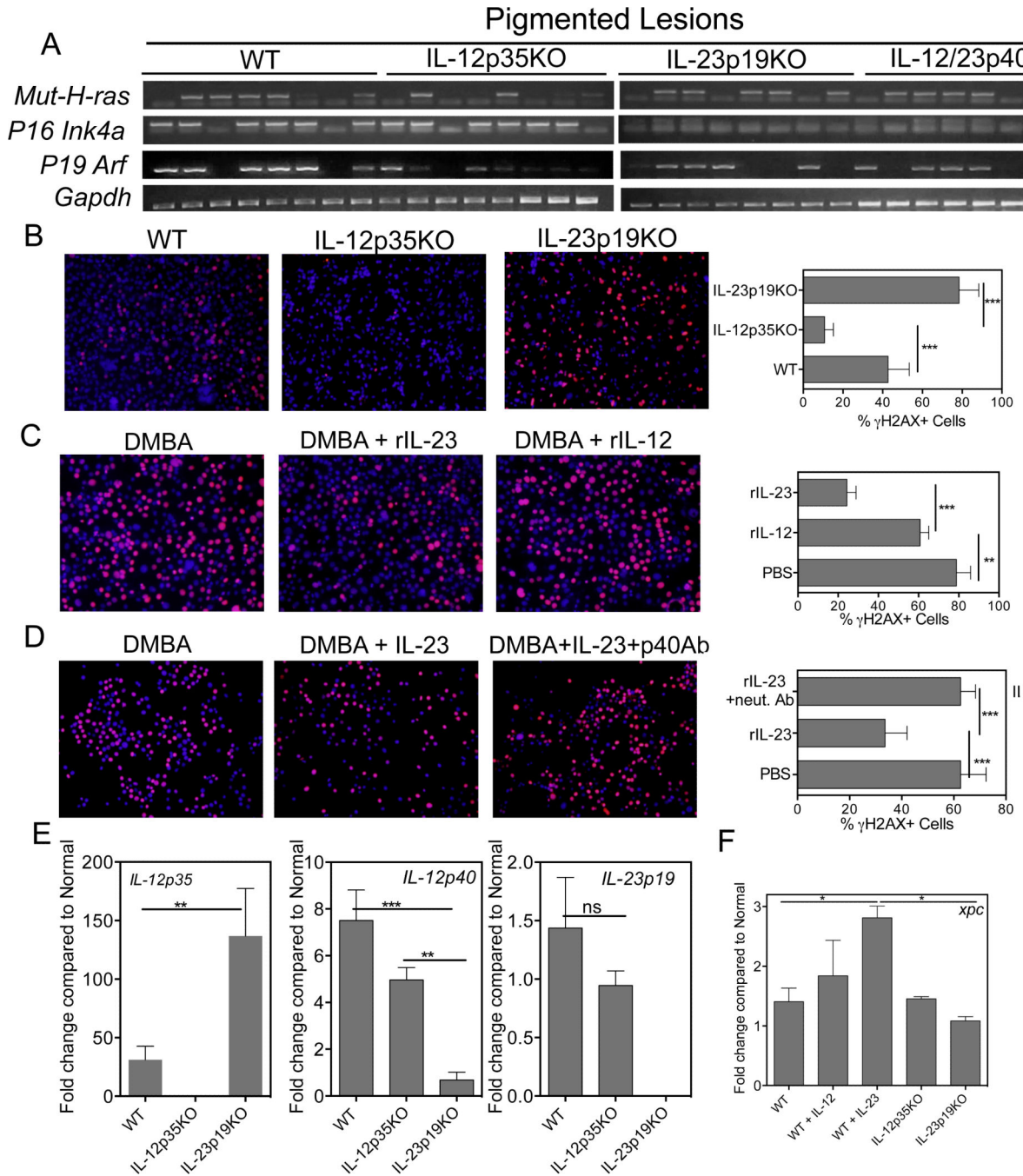
Figure 4. IL-23 reduces genetic instability and induces robust DNA repair in melanocytes
(A) Selective loss of p16INK4a-p19ARF expression and increased H-ras mutations in
IL-23p19KO cell lines. PCR specific primers detecting mutant H-ras(Q61L) and p16Ink4a
and p19Arf expression. White arrows show primer dimers. **(B)** IL-23p19KO melanocytes
were unable to efficiently repair after 24h of DMBA treatment as analyzed by γH2AX
staining (red). Nuclei were stained using DAPI (blue). IL-12p35KO melanocytes repaired
faster than WT or IL-23p19KO melanocytes indicating that IL-12 is not necessary for repair
in melanocytes. **(C)** rIL-23 induces more efficient repair in melanocytes than rIL-12. **(D)**

Addition of neutralizing IL-12p40 antibody inhibited repair mediated by addition of exogenous IL-23 confirming the role of IL-23 in DNA repair. Bars in C, D, & E, represent 5 -7 frames from triplicates. All cells as well as γH2AX positive cells counted and percent damaged cells were calculated by using formula as Percent γH2AX cells =(number of γH2AX positive cells /Total cells) × 100. **(E)** Real-time qPCR analysis of melanocytes that were treated with DMBA for 12h. Cells were collected, RNA extracted as described in Materials and Methods. The bars are plotted as fold change against normal WT melanocytes that received DMSO and no DMBA. **(F)** Real-time qPCR analysis of DNA repair enzyme XPC in melanocytes that were treated with DMBA or DMBA + rIL-12 or rIL-23 for 12h. Cells were collected, RNA extracted as described in Materials and Methods. The bars are plotted as fold change against normal WT melanocytes that received DMSO and no DMBA. ** is $p<0.01$. ***is $p<0.001$. Data is from one experiment representative of two independent experiments.
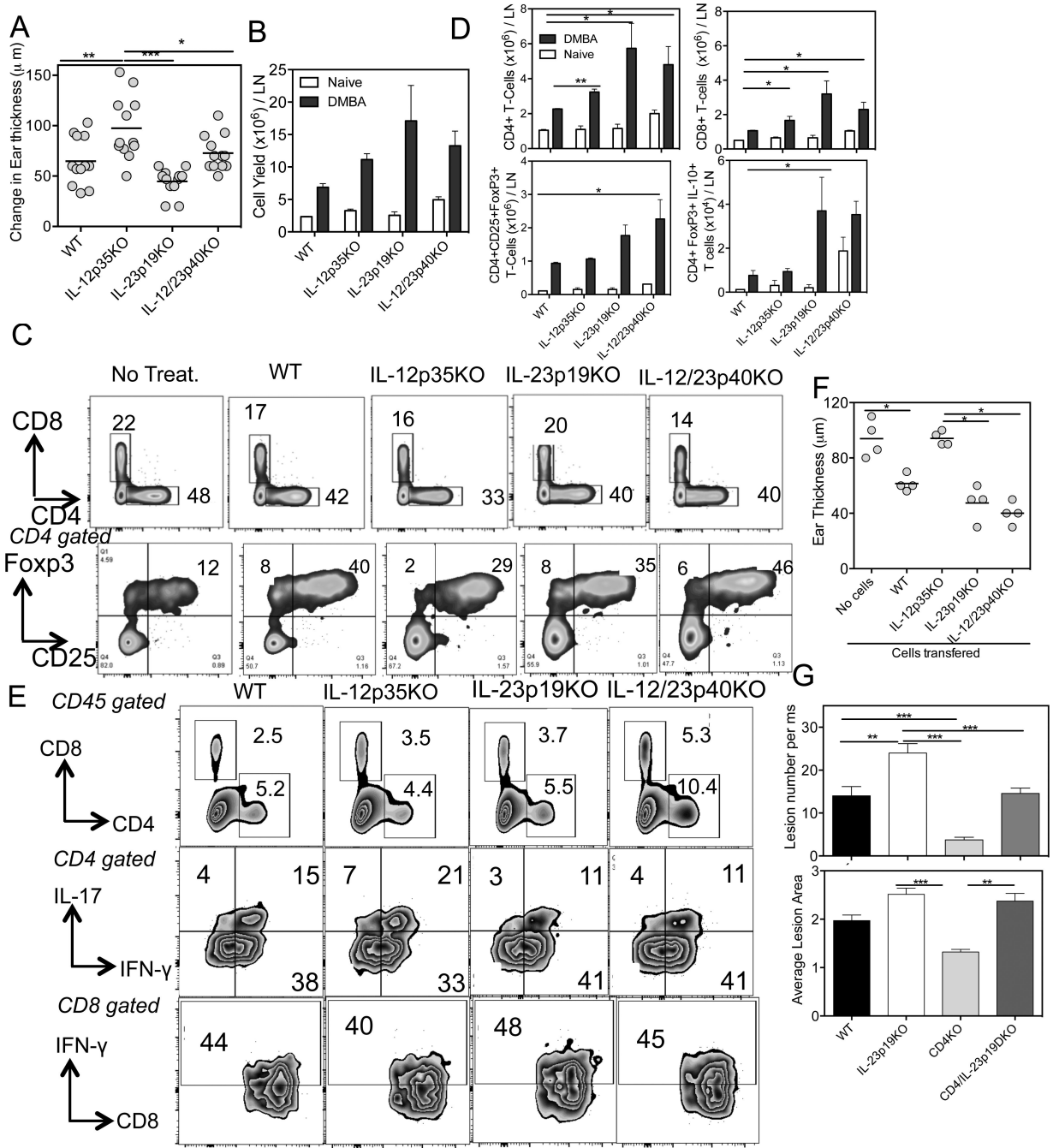
Figure 5. IL-12 normally promotes development of regulatory T-cells that are induced by DMBA
(A) CHS ear swelling responses to DMBA. Allergic contact hypersensitivity responses to DMBA is augmented in IL-12p35KO mice and suppressed in IL-23p19KO mice. This is combination of two independent experiments with both ears and 3 mice each. (B) Total cell yields before and after DMBA challenge in each group of mice. (C) Bivariate contour plot displays of LN subsets. The percent CD4 and CD8 T cells (upper panel) and CD4 gated CD25+Foxp3+ T-cells in all groups (lower panel) are shown. **(D) Absolute cell subset numbers per LN.** IL-23p19KO and IL-12/23p40KO mice showed enhanced CD4, CD8 &

regulatory T cell numbers compared to WT and IL-12p35KO mice. Further, a large number of regulatory T cells produced IL-10 in IL-23p19KO mice than either WT or IL-12p35KO mice. (E) Bivariate displays of skin infiltrating leukocytes, gated by CD45 staining. Cells were isolated from ear skin 3 days after DMBA challenge and subset frequencies determined for each group, as shown. The data is from 3 mice from a single experiment. (F) CHS suppression assay by adoptive transfer of sensitized CD4 T cells. CD4 T cells from DMBA sensitized KO or WT mice, as indicated, were adoptively transferred into previously DMBA sensitized WT mice, then challenged with DMBA on ear skin. Ear swelling was significantly inhibited in mice that received WT, IL-23p19KO and IL-12/23p40KO CD4 T cells, but unaffected by IL-12p35KO CD4 T cells. (G) Altered nevus development in single and double KOs for CD4 and IL-23. The incidence of nevi in CD4 KO mice is reduced by ~ 75%, and increases by almost 50% in IL-23p19KO mice but is at intermediate, WT levels in the DKO mice. However, the average lesion size in DKO mice is similar to single IL23KO mice, suggesting a dominant role for loss of IL-23 control. 10 mice were used in a single experiment. *p is <0.05. ** is p<0.01. ***is p<0.001.
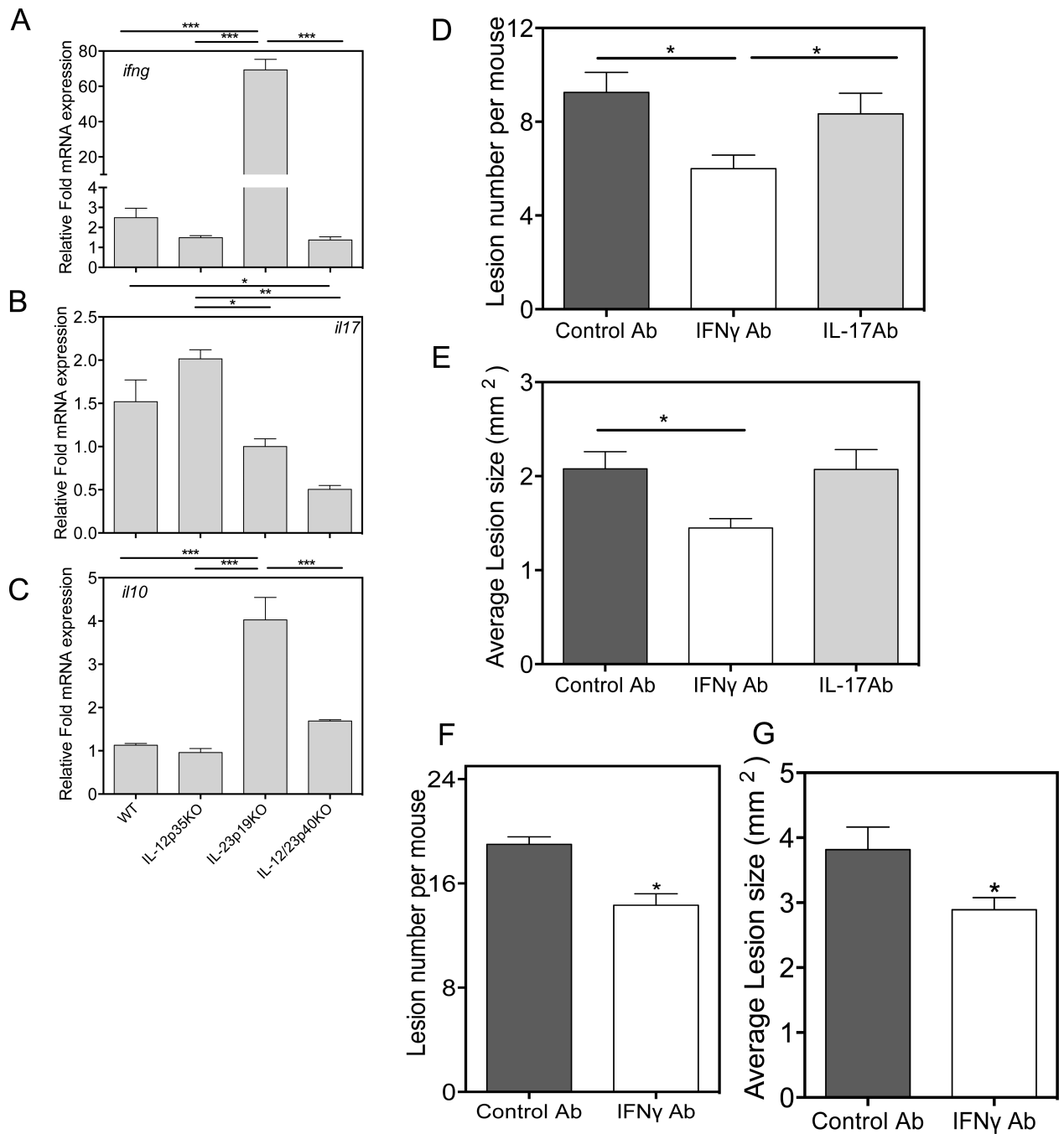
Figure 6. IL-23 inhibits induction of IFNγ gene expression
Real-time PCR analysis of (**A**) IFN-γ (**B**) IL-17 and (**C**) IL-10 using whole skin that was
treated with TPA for 24h. WT and IL-23p19KO mice were treated with DMBA and TPA
with injection of rat isotype antibody, anti-IL-17 and anti-IFN-γ antibodies for 5 weeks after
initial treatment with DMBA. (**D & E**) Number of nevi and average lesion area in WT mice
after mice received anti-IFNγ antibody and IL-17 antibody. (**F & G**) Number of nevi and
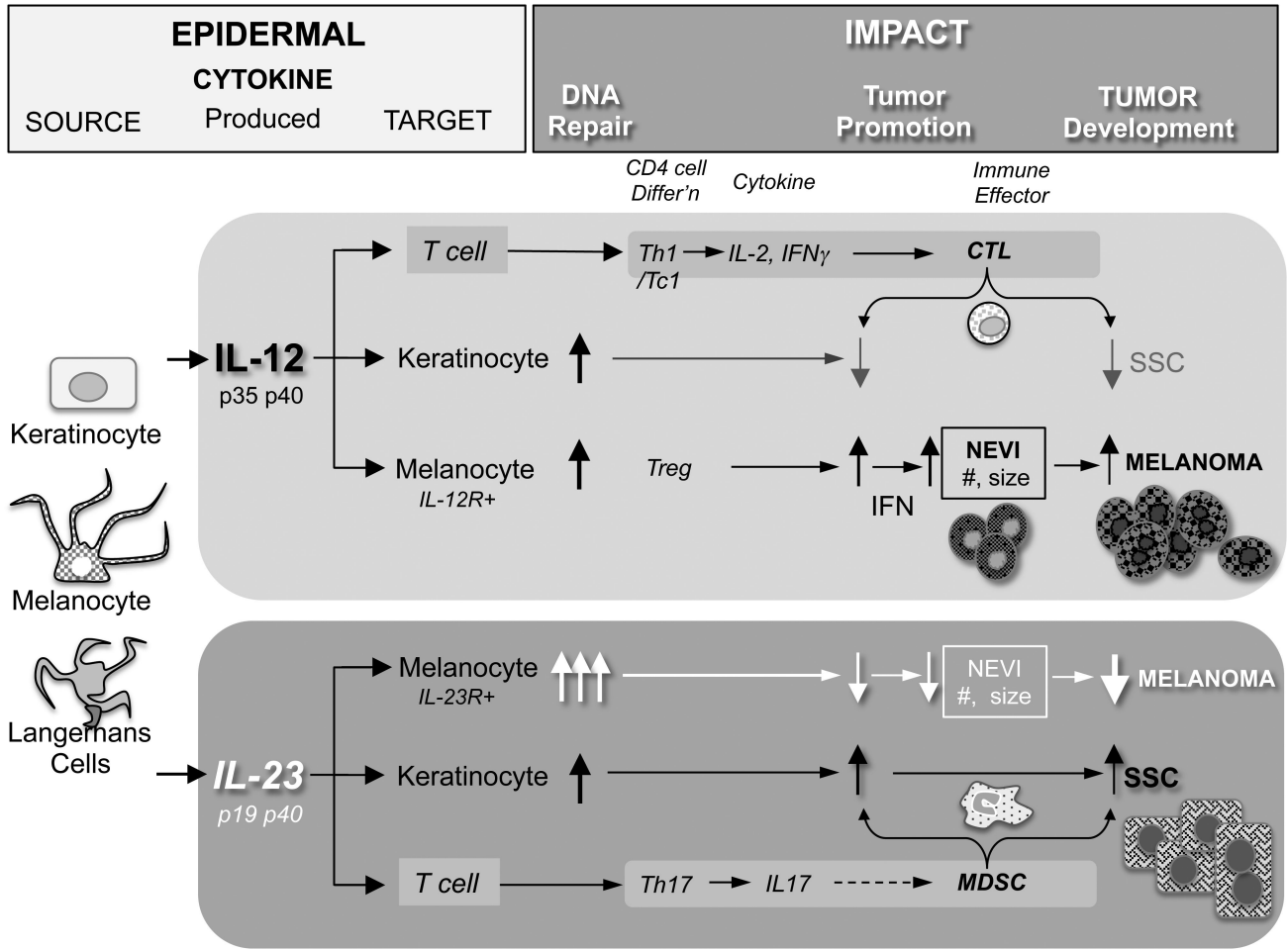average lesion area in IL-23p19KO mice was reduced when mice were injected with anti-

IFNγ antibody. 5 mice were used to in a single experiment. *p is <0.05. ** is p<0.01. ***is p<0.001.

Figure 7. Summary of role of IL-23 in SCC and Melanoma development
DMBA (mutagen) introduces mutations in cells such as keratinocytes (KCs) and melanocytes (MCs). These cells along with Langerhans cells (LCs) secrete the cytokines IL-12 and IL-23. The cytokines can act in an autocrine or paracrine fashion and induce DNA repair. IL-23 augments DNA repair in melanocytes thereby preventing excess mutations in the cells. IL-12 increases IFN production by innate cells as well as T-cells resulting in fewer SCCs due to enhanced CTL. However, high IFN production results in malignant melanocyte proliferation, angiogenesis and melanoma development. IL-23 on the other hand reduces IFN production and increases DNA repair, thus resulting in fewer nevi. IL-23 promotes IL-17 production increases Myeloid Derived Suppressor Cells (MDSCs) in SCCs thus promoting IL-23 mediated SCC development.